TECHBRIEF

# Impact of Initial Density on Strength-Deformation Characteristics of Open-Graded Aggregates

FHWA Publication No. FHWA-HRT-18-048

FHWA Contact: Jennifer Nicks, HRDI-40, (202) 493-3075, jennifer.nicks@dot.gov

## Introduction

Crushed, manufactured open-graded aggregates (OGAs) are often used as structural backfill materials for retaining walls, bridge foundations, and pavement bases because of their engineering properties and general easiness to work with in construction. These attributes can lead to better long-term performance of geotechnical and pavement structures. Specifying OGAs for a highway project is typically based on the American Association of State Highway and Transportation Officials (AASHTO) M 43 gradation, which provides standard sizes for processed aggregates; the equivalent ASTM standard is D448 (AASHTO 2005, ASTM 2011).

During the design process, the shear strength of these materials is often assumed in lieu of testing the material prior to construction; however, a study conducted by the Federal Highway Administration on common AASHTO M 43 OGAs found that the strength of these backfills is considerably greater than the typical default design value of 34 degrees (Nicks et al. 2015). The measured strengths presented by Nicks et al. (2015) were based on the large-scale direct shear (LSDS) and large-diameter triaxial (LDTX) tests performed on AASHTO OGAs ranging from a size number (No.) 5s to 10s, which were compacted at 30-percent relative density (RD). A low RD was selected to provide a conservative estimate,

U.S. Department of Transportation
Federal Highway Administration

Research, Development, and Technology
Turner-Fairbank Highway Research Center
6300 Georgetown Pike
McLean, VA 22101-2296

www.fhwa.dot.gov/research

assuming no compaction; however, in the field, OGAs are compacted during construction, which should yield a higher shear strength.

To investigate the strength-deformation characteristics of OGAs under common conditions in the field (at least 95-percent RD), additional testing was performed, which is described herein. A comparison between low and high RD is also presented, and a new default friction angle is proposed in lieu of testing. These results will help designers make more informed decisions on the range of friction angles that are appropriate for crushed, manufactured OGAs, leading to more reliable and cost-effective designs.

## Previous Work

The factors that govern the strength and deformation behavior of granular materials and aggregates can be categorized as intrinsic or external. Mineralogy and shape aspects, such as angularity, sphericity, and roughness of the individual grains, are examples of intrinsic factors, whereas in-place density, confining stress, pore-water content and its chemistry, and temperature are external factors. Of these aspects, the initial in-place density and the confining stress are two major external factors that have a significant impact on the performance of noncohesive materials.

There is a broad range of information available on the influence of density and confining stress on granular materials; however, most of the studies are focused on small-sized sand materials on which the tests can be conducted using conventional methods. Research by Lee and Seed (1967) is one of the most widely cited works on the drained strength characteristics of sands. In that study, the effect of a wide range of initial densities as functions of various confining stress levels (from about 14 to 1,700 psi) on the shear behavior of a fine, uniform sand was investigated using a triaxial device. The results indicated that the effect of density on strength was more pronounced in very low ranges of stress levels. Also, the denser samples exhibited higher friction angles due to dilation. This relationship between measured friction angles and dilatancy in terms of density has been proven for other types of sands and sand–gravel mixtures using triaxial and other testing devices (Dai et al. 2016, Fragaszy et al. 1992, Hamidi et al. 2009a, 2009b, 2012, Igwe et al. 2012, Novoa-Martinez 2003, Park et al. 2008, Schanz and Vermeer 1996, Sevi 2008, Simoni and Houlsby 2006, Wichtmann and Triantafyllidis 2009, Wijewickreme 1986).

On the strength testing of larger aggregates, there is limited information, which has mainly been focused on rockfill materials (e.g., Al-Hussaini (1983) and Xiao et al. (2014, 2015, 2016)), pavement-base courses (e.g., Theyse (2002)), and railway ballast (e.g., Ionescu (2004) and Raymond and Davies (1978)). Limited information is available on the strength of OGAs specified per the AASHTO M 43 standard: Duncan et al. (2007), Gebrenegus et al. (2015), Knierim (2015), and Nicks et al. (2015). Out of those, Duncan et al. tested a No. 57 aggregate at densities ranging from about 65- to 95-percent RD and found that density did not have a major influence on strength; however, Gebrenegus et al., who studied a wider range of densities (30- and 95-percent RD), found that, for No. 6 and No. 8 aggregates, the densest samples exhibited higher strength characteristics than the loose samples.

While density appears to play a role in peak strength, the work by Sevi (2008) found that there was very little difference in the critical-state friction angle. Wijewickreme (1986) had similar results in his study, finding that the critical-state friction angle was independent of confining pressure, initial density, and particle size; any particle crushing due to testing had a negligible influence. The critical-state friction angle, also known as the constant volume (CV) friction angle, is the strength of the soil/aggregate

Figure 1. Graphs. Gradation curves for the five OGAs tested.

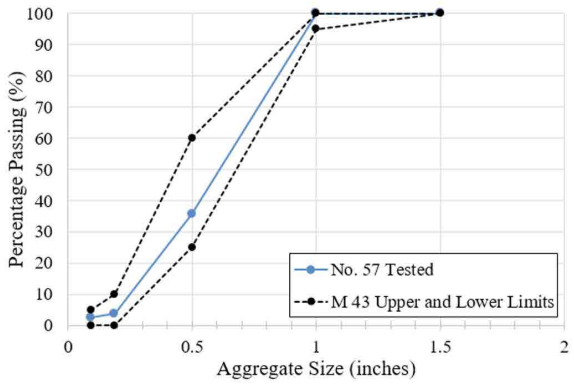


A. No. 57 gradation.

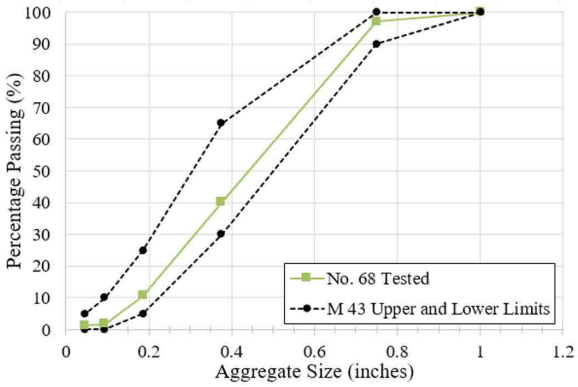


B. No. 68 gradation.

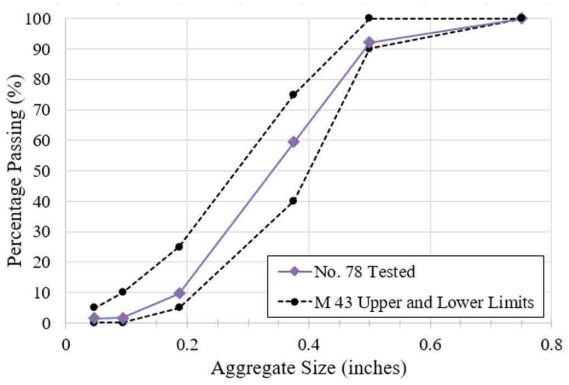


C. No. 78 gradation.

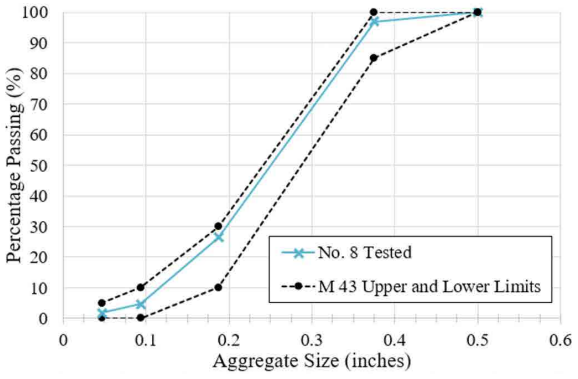


D. No. 8 gradation.

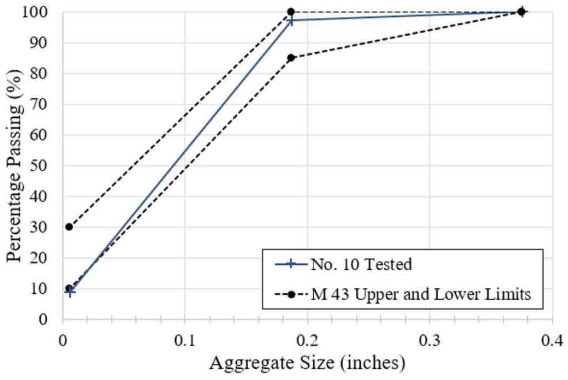


E. No. 10 gradation.

Source for subfigures: FHWA.

postpeak after large deformations. It can be considered a strength-limit parameter, whereas the peak friction angle would be more akin to a service limit.

## OGA Testing Program

In this study, five common AASHTO M 43 aggregates were tested per ASTM D3080 for the LSDS tests and per ASTM D7181 for the LDTX tests: No. 57, No. 68, No. 78, No. 8, and No. 10 (table 1) (ASTM 2004, 2011). The measured gradations of the aggregates from a sieve analysis are shown in figure 1. All the aggregates consist of a crushed diabase rock from the same quarry.

The minimum and maximum dry unit weights for the aggregates were determined using the funnel (Method A of ASTM D4254) and vibratory table (Method 1A of ASTM D4253) methods; the results are shown in table 2. Using the information in table 2, the amount of backfill required for 30- (i.e., loose) and 95-percent (i.e., dense) RD for each test was determined. In the field, compaction control for OGAs is typically a method-based specification, such as compact to nonmovement or no appreciable displacement and assess with visual inspection (Adams and Nicks 2018).

To evaluate the effect of in-place density on the shear strength of these materials, the LSDS and LDTX tests were conducted on five aggregates at both 30- and 95-percent RD. Note that the actual density of the entire sample may not be uniform throughout the entire height with slight variations occurring with each lift of compaction. Similar trends would be found in the field as well where the bottom layer may be denser than the top layer, so this impact is considered inherent and is not a focus of

Table 1. Selected AASHTO M 43-05 (ASTM D448) aggregate designations (shown in terms of percent passing).

| Sieve Size | No. 57 | No. 68 | No. 78 | No. 8 | No. 10 |
|---|---|---|---|---|---|
| 1.5 inches | 100 | - | - | - | - |
| 1 inch | 95–100 | 100 | - | - | - |
| 0.75 inch | - | 90–100 | 100 | - | - |
| 0.50 inch | 25–60 | - | 90–100 | 100 | - |
| 0.375 inch | - | 30–65 | 40–75 | 85–100 | 100 |
| No. 4 | 0–10 | 5–25 | 5–25 | 10–30 | 85–100 |
| No. 8 | 0–5 | 0–10 | 0–10 | 0–10 | - |
| No. 16 | - | 0–5 | 0–5 | 0–5 | - |
| No. 50 | - | - | - | - | - |
| No. 100 | - | - | - | - | 10–30 |

-Not applicable

Table 2. Unit weight of aggregates and required backfill amounts for 30- and 95-percent RD.

| Sample | Minimum (pcf) | Maximum (pcf) | Amount of Required Backfill/ Test (lbs) LSDS Test | | Amount of Required Backfill/ Test (lbs) LDTX Test | |
|---|---|---|---|---|---|---|
| | | | 30% RD | 95% RD | 30% RD | 95% RD |
| No. 57 | 96.0 | 108.7 | 62.6 | 67.5 | 19.7 | 21.2 |
| No. 68 | 96.2 | 115.9 | 63.3 | 71.7 | 19.9 | 22.5 |
| No. 78 | 102.5 | 118.2 | 66.7 | 73.3 | 20.9 | 23.0 |
| No. 8 | 98.4 | 112.8 | 63.9 | 70.0 | 20.1 | 22.0 |
| No. 10 | 116.4 | 146.3 | 77.5 | 90.3 | 24.4 | 28.4 |

Figure 2. Photos. LSDS and LDTX devices.

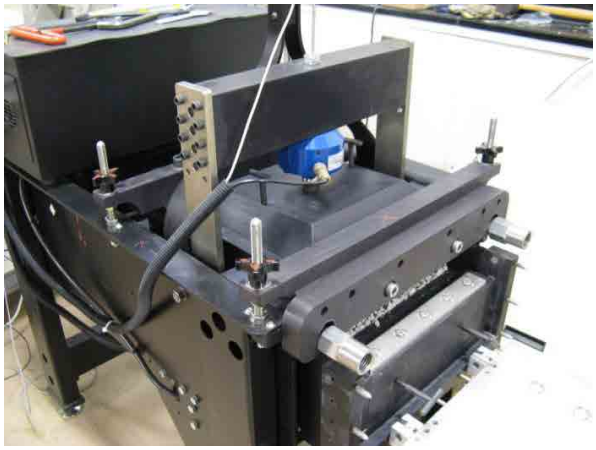

A. LSDS device.

B. LDTX device.

Source for subfigures: FHWA.

this study. The LSDS device consisted of a 12- by 12- by 8-inch box (figure 2-A), and the LDTX device holds a 6-inch-diameter specimen (figure 2-B).

## LSDS Testing Procedure

The gap between the top and bottom shear boxes for each sample was set to $d_{85}$ (the aggregate size in which 85 percent of the material is smaller) based on the sieve analysis (figure 1), and the shear strain displacement rate was set at 0.015 inch/min based on information obtained during the consolidation phase for the aggregates. Each aggregate was tested at four normal stresses: 5, 10, 15 and 30 psi.

To place the aggregates in the shear box at 30- and 95-percent RD, the samples were

packed in three and five lifts, respectively. Each lift was tapped using a wooden pestle until the target lift thicknesses of 2.5 and 1.5 inches were achieved for the loose and dense compaction states, respectively. All the tests were performed under dry conditions; previous work indicated that shear strength and deformation behaviors of OGAs were relatively insensitive to the degree of saturation (Nicks et al. 2015). The load cells and linear variable differential transformers on the LSDS device were calibrated for displacements, loads, and shear track resistance prior to testing.

## LDTX Testing Procedure

Similar to the LSDS tests, the LDTX tests were conducted at 30- and 95-percent RD at confining stresses of 5, 15, and 30 psi. The information in table 2 was used to prepare the 6-inch-diameter by 12-inch-high samples. The samples at 30-percent RD were prepared by compacting three 4-inch layers. Each layer consisted of pouring a predetermined aggregate mass into the split mold through a funnel with a near-zero drop height. The 95-percent RD samples were prepared in six 2-inch layers. Each layer was hand tamped with a wooden pestle until the aggregates settled to the desired height. The samples were prepared with two latex membranes; the inner membrane was considered sacrificial because the compaction of coarse aggregates often punctures the membrane. The results were calculated using the appropriate membrane correction factor.

Stability of the sample throughout the preparation phase was maintained by applying partial suction to the sample through one of the drainage valves located on the base of the testing pedestal. After mounting the specimens on the load frame, the samples were initially presatured via gravity to facilitate the saturation phase and minimize the supply of water from the pumps. The test procedure included a back pressure–saturation method to achieve the acceptable minimum Skempton's B value of 0.95. Following the saturation phase, the samples were isotropically consolidated to the target effective confining pressure before the initiation of the strain-controlled shear step. The imposed strain rate was selected based on the estimated time needed to achieve 90 percent of the total consolidation. Detailed testing procedures and approaches used for data corrections and extracted parameters from the data analysis were previously reported in Nicks et al. (2015).

## Results and Analysis

The key parameters evaluated in this report were the secant and tangent friction angles, maximum dilation angle, and CV friction angle for each aggregate tested.

### Friction Angles

The secant friction angles obtained from the LSDS and LDTX tests for the aggregates at both 30- and 95-percent RD are shown in table 3 and table 4, respectively. For the LSDS results, secant friction angles increased between 5 and 53 percent when compacted at a higher state, with an average increase of 23 percent. For the LDTX results, the increase was not as pronounced, with an average increase of about 16 percent. The biggest difference occurred for the No. 10 aggregate, and the smallest difference occurred for the No. 57 aggregate. This is likely a result of the void ratio

Table 3. Results of LSDS secant friction angles (in units of degrees).

| AASHTO Classification | 5 psi | | 10 psi | | 5 psi | | 30 psi | |
|---|---|---|---|---|---|---|---|---|
| | 30% RD | 95% RD | 30% RD | 95% RD | 30% RD | 95% RD | 30% RD | 95% RD |
| No. 57 | 70.6 | 73.8 | 65.4 | 73.3 | 60.8 | 71.6 | 55.5 | **61.4** |
| No. 68 | 64.1 | 77.8 | 60.3 | 74.8 | 60.0 | 73.3 | 56.4 | 68.7 |
| No. 78 | 65.6 | 76.4 | 62.5 | 70.7 | 60.7 | 71.1 | 55.8 | 65.8 |
| No. 8 | 67.0 | 75.5 | 65.4 | 74.2 | 62.4 | 67.8 | 56.2 | 64.2 |
| No. 10 | 50.7 | 75.0 | 45.3 | 73.3 | 45.9 | 68.8 | 41.8 | 63.9 |

Table 4. Results of LDTX secant friction angles (in units of degrees).

| AASHTO Classification | 5 psi | | 15 psi | | 30 psi | |
|---|---|---|---|---|---|---|
| | 30% RD | 95% RD | 30% RD | 95% RD | 30% RD | 95% RD |
| No. 57 | 46.3 | 53.5 | 41.4 | 46.3 | 39.0 | 42.1 |
| No. 68 | 45.2 | 53.7 | 42.1 | 49.1 | 38.9 | 45.1 |
| No. 78 | 43.5 | 43.5 | 42.0 | 50.4 | 39.6 | 47.9 |
| No. 8 | 43.2 | 49.5 | 38.5 | 46.1 | 37.6 | 43.2 |
| No. 10 | 45.3 | 53.3 | 41.8 | 51.6 | 41.1 | 49.1 |

of the aggregates; the No. 57 aggregate had a large amount of void space relative to the No. 10. The difference between the minimum and maximum densities was smallest for the No. 57 aggregate and largest for the No. 10 (table 2). As anticipated, the secant friction angle decreased with increasing confining pressure because the confinement suppressed dilation.

While there is a difference between the LSDS and LDTX tests under both loose and dense conditions, the trend for the secant friction angles is consistent for each aggregate (figure 3). There is a linear relationship in the results between the two test devices. The slope of the lines for each aggregate generally ranges from 1.2 to 1.5 when fit to a 0 intercept (table 5). The closest result between the LSDS and LDTX tests occurred for the No. 10 aggregates. While the No. 10 is of the same mineralogy, its coefficient of uniformity (*Cu*) is considerably higher than the other aggregates (table 5), behaving more like a well-graded aggregate. This suggests that the difference between the LSDS and LDTX results may narrow as the gradation becomes less uniform; however, the limited data set in this study prevents a definitive conclusion.

Under the confining pressures tested for each sample, the tangent friction angles

were also determined assuming a linear Mohr–Coulomb failure envelope (table 6). The friction angles measured at 95-percent RD were expectedly higher than those at 30-percent RD; however, there was no trend with aggregate properties universal to the six aggregates tested (figure 4). This difference could partly be due to the difficulties in defining a single index describing each of the aggregates to be correlated with the measured tangent friction angles. For example, average particle size, coefficient of uniformity, maximum density, etc., can all factor into strength.

As shown in figure 4, the results support the general trend of triaxial testing producing lower friction angles than those found from direct shear testing. At 30-percent RD, the LSDS results are, on average, about 20-percent higher than the LDTX results, while at 95-percent RD, the results from

Figure 3. Graph. Comparison between secant friction angles from the LSDS and LDTX tests.

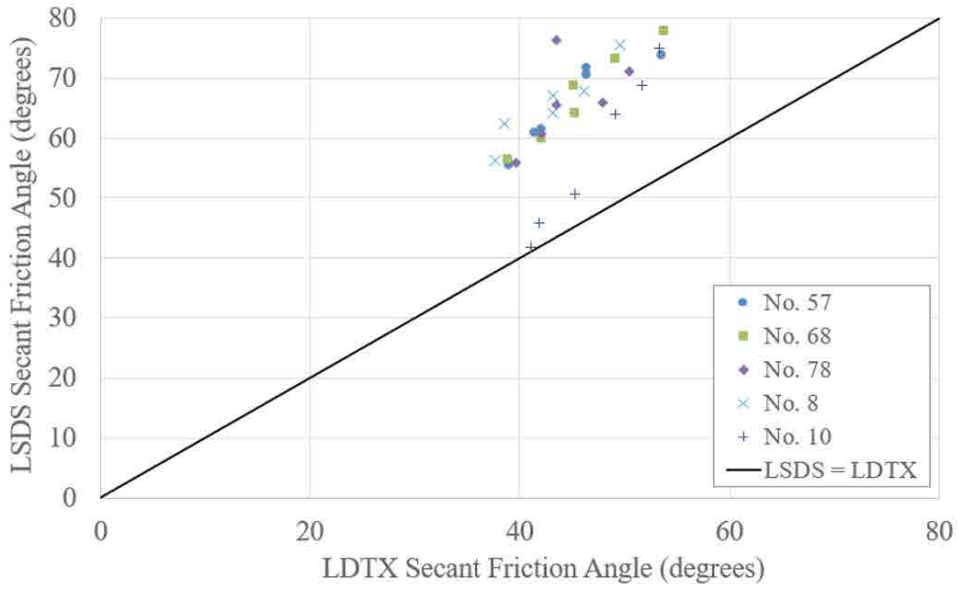


Source: FHWA.

Table 5. Aggregate properties and comparison between the LSDS and LDTX results.

| AASHTO Classification | Average Particle Size $d_{50}$ (Inches) | Coefficient of Uniformity *Cu* | Coefficient of Curvature *Cc* | Ratios for LSDS/ LDTX Secant Friction Angles |
|---|---|---|---|---|
| No. 57 | 0.67 | 1.72 | 1.04 | 1.46 |
| No. 68 | 0.42 | 2.63 | 1.13 | 1.46 |
| No. 78 | 0.34 | 2.01 | 0.98 | 1.50 |
| No. 8 | 0.28 | 0.79 | 0.65 | 1.52 |
| No. 10 | 0.05 | 9.92 | 0.99 | 1.24 |

Table 6. Tangent friction angles from the LSDS and LDTX tests (in units of degrees).

| AASHTO Classification | LSDS | | LDTX | |
|---|---|---|---|---|
| | 30% RD | 95% RD | 30% RD | 95% RD |
| No. 57 | 49.1 | 55.9 | 37.0 | 37.8 |
| No. 68 | 54.3 | 64.7 | 37.2 | 37.2 |
| No. 78 | 52.6 | 61.9 | 38.6 | 43.7 |
| No. 8 | 52.0 | 58.2 | 36.5 | 41.2 |
| No. 10 | 39.7 | 58.4 | 40.6 | 47.8 |

Figure 4. Bar charts. Comparisons of tangent friction angles between 30- and 95-percent RD.

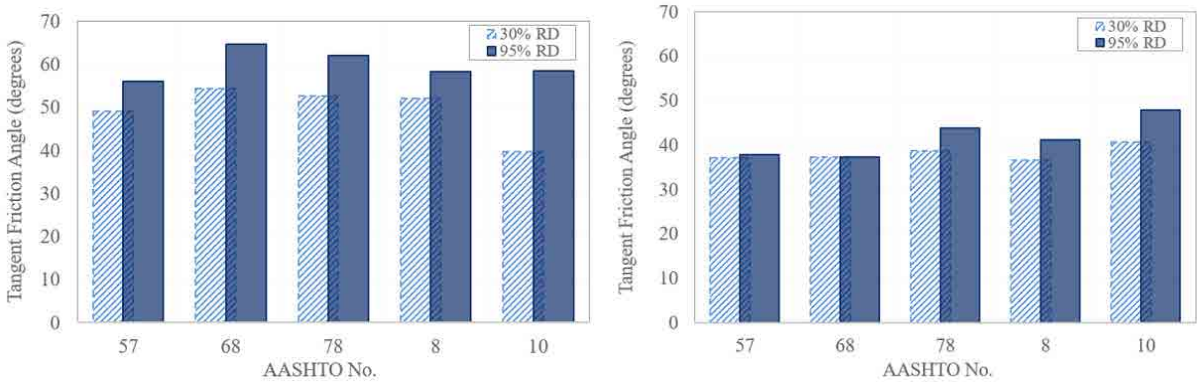


A. LSDS tangent friction angles.

B. LDTX tangent friction angles.

Source for subfigures: FHWA.

direct shear testing are, on average, about 30-percent higher than LDTX results. This indicates that the initial density of the sample also played a role in the difference resulting from testing devices, particularly in the case of the LSDS.

## Maximum Dilation Angle

The maximum dilation angle for each aggregate at each confining stress is presented in table 7 and table 8 for the LSDS and LSTX tests, respectively. Dilation is a contributing component of aggregate strength—with measured higher dilation angles being more common in aggregate tests with higher peak friction angles. As expected, dilation angles are greater in samples prepared at greater RDs due to the reduced void ratio of the sample. Additionally, the measure of the dilation angle is greater in the LSDS test than the LDTX test, which likely has to do with the differences in the boundary conditions between the two devices (Nicks et al. 2015). The rigid boundary of the LSDS promotes mobilization of the aggregates, especially when densely

Table 7. LSDS dilation angles (in units of degrees).

| AASHTO Classification | 5 psi | | 10 psi | | 5 psi | | 30 psi | |
|---|---|---|---|---|---|---|---|---|
| | 30% RD | 95% RD | 30% RD | 95% RD | 30% RD | 95% RD | 30% RD | 95% RD |
| No. 57 | 17.7 | 19.8 | 10.7 | 18.8 | 10.2 | 17.1 | 7.5 | 9.0 |
| No. 68 | 14.9 | 24.2 | 9.0 | 20.2 | 6.8 | 17.8 | 6.9 | 18.3 |
| No. 78 | 12.7 | 26.4 | 11.5 | 24.5 | 12.6 | 21.4 | 7.6 | 16.3 |
| No. 8 | 15.9 | 25.6 | 12.5 | 21.1 | 12.9 | 16.5 | 6.6 | 12.0 |
| No. 10 | 3.4 | 27.6 | 1.7 | 20.2 | 2.1 | 20.8 | 0.0 | 16.4 |

Table 8. LDTX dilation angles (in units of degrees).

| AASHTO Classification | 5 psi | | 15 psi | | 30 psi | |
|---|---|---|---|---|---|---|
| | 30% RD | 95% RD | 30% RD | 95% RD | 30% RD | 95% RD |
| No. 57 | 9.4 | 16.3 | 3.4 | 8.9 | 0.0 | 2.4 |
| No. 68 | 7.8 | 16.5 | 3.6 | 12.1 | 0.0 | 6.3 |
| No. 78 | 9.2 | 17.4 | 7.6 | 13.6 | 5.0 | 10.1 |
| No. 8 | 8.5 | 15.8 | 2.6 | 11.0 | 1.5 | 6.2 |
| No. 10 | 6.3 | 14.3 | 2.8 | 11.9 | 4.4 | 9.6 |

Table 9. CV friction angles (in units of degrees).

| AASHTO Classification | LSDS | | LDTX | |
|---|---|---|---|---|
| | 30% RD | 95% RD | 30% RD | 95% RD |
| No. 57 | 47.2 | 51.0 | 38.9 | 39.7 |
| No. 68 | 53.4 | 52.7 | 39.0 | 39.6 |
| No. 78 | 44.5 | 51.1 | 35.0 | 41.2 |
| No. 8 | 48.8 | 53.7 | 36.4 | 39.0 |
| No. 10 | 41.3 | 51.2 | 38.1 | 40.7 |

compacted, whereas the flexible boundary of the LDTX relatively suppresses mobilization and allows for greater freedom to deviate laterally with reduced strength enhancement due to dilatancy (Bolton 1986). Regardless, the difference due to the initial density of the sample becomes larger for the aggregates as the confining stress increases. There is no definitive trend with respect to the aggregate size.

## CV Friction Angle

The linear relationship between the secant friction angle and the maximum dilation angle for an aggregate allows for the estimation of the CV friction angle using the zero-dilation-angle (ZDA) approach; the results for each aggregate are shown in table 9. Theoretically, at the critical state, the CV friction angle should be independent of initial density (Lee et al. 2008; Negussey et al. 1988, Rowe 1962; Wijewickreme 1986). At high surcharge pressures, however, the potential for particle crushing and the associated change in soil gradation may result in lower CV friction angles (Hamidi et al. 2009b). Minimal differences in the CV friction angles were found between the 30- and 95-percent RDs (less than 7 percent); however, there is a more pronounced difference with the LSDS results, ranging from about 10 to 20 percent between the 30- and 95-percent RDs. This suggests that the results from the LSDS device require a broader range of initial densities to determine the CV friction angle.

When combining the results for every aggregate tested at both densities, the same linear trend between the secant friction angle and the maximum dilation angle

Figure 5. Graph. Relationship between friction and dilation angles.

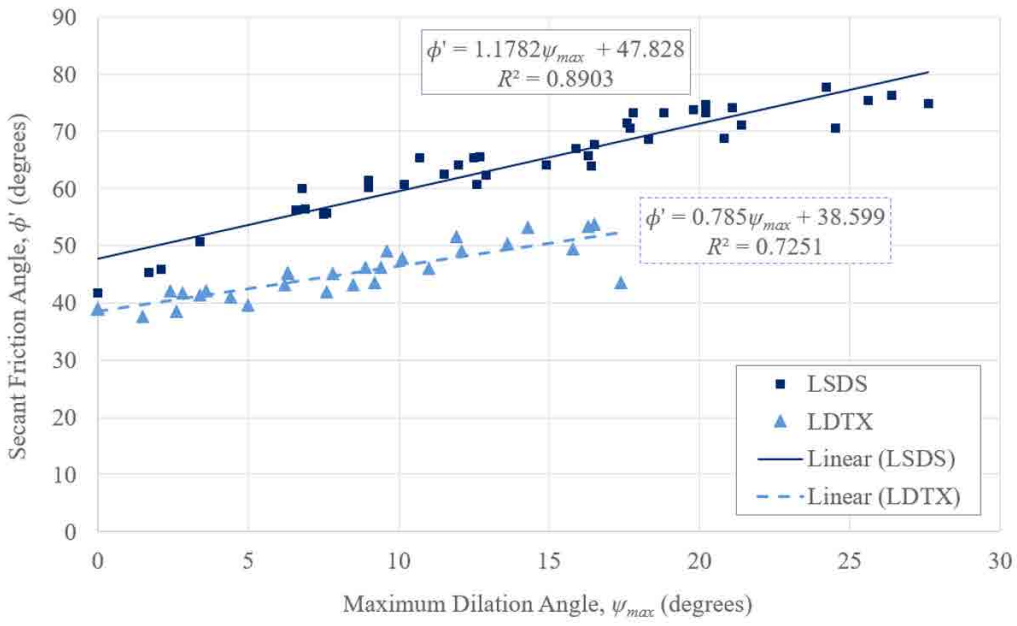


Source: FHWA.

Figure 6. Graph. Estimated versus predicted OGA friction angles using the Bolton (1986) equation for the LSDS and LDTX tests.

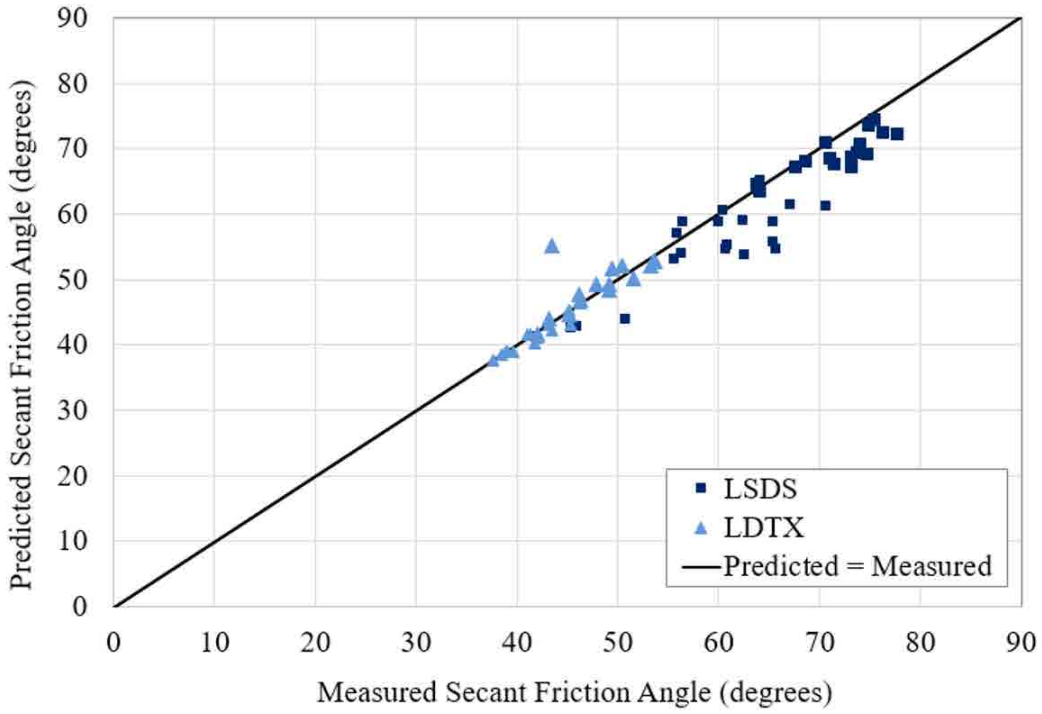


Source: FHWA.

was found (figure 5). Based on this, the ZDA approach gives 48 and 39 degrees as the CV friction angle for LSDS and LDTX testing, respectively. The failure mechanisms that the aggregates experience for structures such as retaining walls and abutments are more closely related to plane strain conditions where the friction angles are widely reported to be higher than from LSDS and LDTX tests. For this reason, the results obtained from this study are considered conservative. For the applications in which OGAs are typically used, and assuming a coefficient of variation of 5 percent (from Paikowsky et al. (2010)) and a 95-percent confidence interval, a proposed, default friction angle of 40 degrees for OGAs as structural backfills is suggested.

## Summary and Conclusions

The analysis of the individual components of the secant friction angle, the CV friction angle, and the maximum dilation angle showed that the results from the direct shear exhibited a significantly increased CV angle and maximum dilation angle, which contributed to the overall higher secant friction angle for LSDS-based tests, notwithstanding the aggregate type, confining stress, and density level. One common transformation used to backcalculate the secant friction angle, CV friction angle, or dilation angle is shown in equation 1, which was presented by Bolton (1986) based on testing results for different sands in axisymmetric and plane strain conditions. The equation was evaluated in this study for the crushed, manufactured OGAs using

the results from both the nonaxisymmetric LSDS testing and the axisymmetric LDTX testing (figure 5).

$$\phi' = \phi'_{CV} + 0.8\psi_{max} \quad (1)$$

Where:

$\phi'$ = maximum secant friction angle.
$\phi'_{CV}$ = CV friction angle.
$\psi_{max}$ = maximum dilation angle.

There is relatively good agreement between the data and equation 1 regardless of the test method, although the LSDS results were more scattered (figure 6). As figure 5 indicates, better agreement for LSDS tests may come with a factor of about 1.2 applied to the measured maximum dilation angle rather than 0.8; however, for a rough, preliminary estimate, equation 1 is sufficient until further testing is performed on these aggregates. It is worth noting that equation 1 suggests a unique CV friction angle; however, the $\phi'_{CV}$ was found to be variable between the LSDS and LDTX results (table 9) suggesting a coefficient may be needed for that component in addition to the coefficient already applied to the dilation angle.

The results of this research indicated that a default friction angle of 40 degrees is appropriate for the crushed, manufactured OGAs studied herein when used as structural backfill for retaining walls and bridge abutments. Additional testing on more samples will refine this value; however, physical testing is still recommended during the design process. Finally, it was found that the Bolton (1986) equation is a good approximation for the relationship between friction and dilation angles of OGAs.

## References


AASHTO. (2005). *M 43: Standard Specification for Sizes of Aggregate for Road and Bridge Construction*, American Association of State Highway and Transportation Officials, Washington, DC.

Adams, M., and Nicks, J. (2018). *Design and Construction Guidelines for Geosynthetic Reinforced Soil Abutments and Integrated Bridge Systems*, Report No. FHWA-HRT-17-080, Federal Highway Administration, Washington, DC.

Al-Hussaini, M. (1983). "Effect of Particle Size and Strain Conditions on the Strength of Crushed Basalt." *Canadian Geotechnical Journal*, 20, 10.1139/t83-077, pp. 706–717.

ASTM D3080. (2004). "StandardTest Method for Direct Shear Test of Soils under Consolidated Drained Conditions." *Annual Book of ASTM Standards*, ASTM International, West Conshohocken, PA.

ASTM D4253. (2006). "Standard Test Methods for Maximum Index Density and Unit Weight of Soils Using a Vibratory Table." *Annual Book of ASTM Standards*, ASTM International, West Conshohocken, PA.

ASTM D4254. (2006). "Standard Test Methods for Minimum Index Density and Unit Weight of Soils and Calculation of Relative Density." *Annual Book of ASTM Standards*, ASTM International, West Conshohocken, PA.

ASTM D448. (2012). "Standard Classification for Sizes of Aggregate for Road and Bridge Construction." *Annual Book of ASTM Standards*, ASTM International, West Conshohocken, PA.

ASTM D7181. (2011). "Method for Consolidated Drained Triaxial CompressionTest for Soils." *Annual Book of ASTM Standards*, ASTM International, West Conshohocken, PA.

Bolton, M. D. (1986). "The strength and dilatancy of sands." *Géotechnique*, 36(1), 10.1680/geot.1986.36.1.65, pp. 65–78, ICE Publishing, Thomas Telford Ltd, Scotland.

Dai, B. B., Yang, J., and Zhou, C. Y. (2016). "Observed Effects of Interparticle Friction and Particle Size on Shear Behavior of Granular Materials." *International Journal of Geomechanics*, 10.1061/(ASCE)GM.1943-5622.0000520, 04015011.

Duncan, J. M., Brandon, T., Jian, W., Smith, G., Park, Y., Griffith, T., Corton, J., and Ryan, E. (2007). *Densities and Friction Angles of Granular Materials with Standard Gradations 21B and #57*, Report CGPR #45, Center for Geotechnical Practice and Research, Virginia Polytechnic Institute, Blacksburg, VA.

Fragaszy, R. J., Su, J., Siddiqi, F. H., and Ho, C. L. (1992). "Modeling Strength of Sandy Gravel." *Journal of Geotechnical Engineering*, 118(6), 10.1061/(ASCE)0733-9410(1992)118:6(920), pp. 920–935.

Gebrenegus, T, Nicks, J., and Adams, M. (2015). "Large Diameter Triaxial Testing of AASHTO Open Graded Aggregates and the Effect of Relative Density on Strength." *Proceedings of the International Foundations Congress and Equipment Expo 2015*, San Antonio, TX.

Hamidi, A., Yazdanjou, V., and Salimi, N. (2009a). "Shear Strength Characteristics of Sand-Gravel Mixtures." *International Journal of Geotechnical Engineering*, 3(1), 10.3328/IJGE.2009.03.01.29-38, pp. 29–38.

Hamidi, A., Alizadeh, A., and Soleimani, S. M. (2009b). "Effect of Particle Crushing on Shear Strength and Dilation Characteristics of Sand-Gravel Mixtures." *International Journal of Civil Engineering*, 7(1), pp. 61–71.

Hamidi, A., Azini, E., and Masoudi, B. (2012). "Impact of Gradation on the Shear Strength-Dilation Behavior of Well Graded Sand-Gravel Mixtures." *Scientia Iranica*, 19(3), 10.1016/j.scient.2012.04.002, pp. 393–402.

Igwe, O., Fukuoka, H., and Sassa, K. (2012). "The Effect of Relative Density and Confining Stress on Shear Properties of Sands with Varying Grading." *Geotechnical and Geological Engineering*, 30(5), 10.1007/s10706-012-9533-2, pp. 1,207–1,229.

Ionescu, D. (2004). *Evaluation of the Engineering Behavior of Railway Ballast*, PhD Dissertation, University of Wollongong, New South Wales, Australia.

Knierim, C. D. (2015). *Geotechnical Characterization and Drained Shear Strength of a Limestone*, BSc Thesis, Oregon State University, Corvallis, OR.

Lee, J., Eun, J., Lee, K., Park, Y., and Kim, M. (2008). "In-Situ Evaluation of Strength and Dilatancy of Sands Based on CPT Results." *Soils and Foundations*, 48(2), 10.3208/sandf.48.255, pp. 261–271.

Lee, K. L. and Seed, H. B. (1967). "Drained Strength Characteristics of Sands." *Journal of the Soil Mechanics and Foundation Division*, 93(6), pp. 117–141.

Negussey, D., Wijewickreme, W. K. D., and Vaid, Y. P. (1988). "Constant-Volume Friction Angle of Granular Materials." *Canadian Geotechnical Journal*, 25(1), 10.1139/t88-006, pp. 50–55.

Nicks, J. E., Gebrenegus, T., Adams, M. T. (2015). *Strength Characterization of Open-Graded Aggregates for Structural Backfills*, FHWA-HRT-15-034, Federal Highway Administration, Washington, DC.

Novoa-Martinez, B. (2003). *Strength Properties of Granular Materials*, MSc Thesis, Louisiana State University, Baton Rouge, LA.

Paikowsky, S. G., Canniff, M. C., Lesny, K., Kisse, A. Amatya, S., and Muganga, R. (2010). *LRFD Design and Construction of Shallow Foundations for Highway Bridge Structures*, NCHRP Report 651, Transportation Research Board, Washington, DC.

Park, L. K., Suneel, M., and Chul, I. J. (2008). "Shear Strength of Jumunjin Sand According to Relative Density." *Marine Georesources and Geotechnology*, 26(2), 10.1080/10641190802022445, pp. 101–110.

Raymond, G. P., and Davies, J. R. (1978). "Triaxial Tests on Dolomite Railroad Ballast." *Journal of the Geotechnical Engineering Division*, 104(6), pp. 737–751.

Rowe, P. W. (1962). "The Stress-Dilatancy Relation for the Static Equilibrium of an Assembly of Particles in Contact." *Proceedings of the Royal Society London, Series A. Mathematical and Physical Sciences*, 269(1339), 10.1098/rspa.1962.0193, pp. 500–527.

Theyse, H. L. (2002). *Stiffness, Strength, and Performance of Unbound Aggregate Material: Application of South African HVS and Laboratory Results to California Flexible Pavement*, University of California Pavement Research Center, Davis, CA.

Schanz, T. and Vermeer, P. A. (1996). "Angles of Friction and Dilatancy of Sand." *Geotechnique*, 46(1), 10.1680/geot.1996.46.1.145, pp. 145–151.

Sevi, A. F. (2008). *Physical Modeling of Railroad Ballast Using the Parallel Gradation Scaling Technique within the Cyclical Triaxial Framework*, PhD Thesis, Missouri University of Science and Technology, Rolla, MO.

Simoni, A. and Houlsby, G. T. (2006). "The Direct Shear Strength and Dilatancy of Sand-Gravel Mixtures." *Geotechnical and Geological Engineering*, 24, 10.1007/s10706-004-5832-6, pp. 523–549.

Wichtmann, T. and Triantafyllidis. (2009). "On the correlations of 'static' and 'dynamic' stiffness moduli of non-cohesive soils." *Bautechnik 86, Issue S1: Geotechnical Engineering*, 10.1002/bate.200910039, pp. 28–39.

Wijewickreme, D. (1986). *Constant Volume Friction Angle of Granular Materials*, MSc Thesis, University of British Columbia, Vancouver, Canada.

Xiao, Y., Liu, H., Chen, Y., and Jiang, J. (2014). "Strength and Deformation of Rockfill Material Based on Large-Scale Triaxial Compression Tests. I: Influences of Density and Pressure." J*ournal of Geotechnical and Geoenvironmental Engineering*, 10.1061/(ASCE)GT.1943-5606.0001176, 04014070.

Xiao, Y., Liu, H., Chen, Y., Jiang, J., and Zhang, W. (2015). "State-Dependent Constitutive Model for Rockfill Materials." *International Journal of Geomechanics*, 10.1061/(ASCE)GM.1943-5622.0000421, 4014075.

Xiao, Y., Liu, H., Zhang, W., Liu, H., Yin, F., and Wang, Y. (2016). "Testing and Modeling of Rockfill Materials: A Review." *Journal of Rock Mechanics and Geotechnical Engineering*, 8, 10.1016/j.jrmge.2015.09.009, pp. 415–422.

**Researchers**—This research was conducted by Jennifer Nicks (HRDI-40) and Michael Adams (HRDI-10) from FHWA, with support from Thomas Gebrenegus from Engineering & Software Consultants through DTFH6117D00011.

**Distribution**—This TechBrief is being distributed according to a standard distribution. Direct distribution is being made to the Divisions and Resource Center.

**Availability**—This TechBrief may be obtained from the FHWA Product Distribution Center by e-mail to report.center@dot.gov, fax to (814) 239-2156, phone to (814) 239-1160, or online at http://www.fhwa.dot.gov/research.

**Key Words**—Aggregates, laboratory testing, large-scale direct shear, AASHTO, materials, friction angle, dilation angle, constant volume



AUGUST 2018

FHWA-HRT-18-048
HRDI-40/08-18(WEB)E